CrossMark

Vacuolar ATPase driven potassium transport in highly metastatic breast cancer cells

Sarah A. Salyer [a,b], Jordan R. Olberding [a], Anthony A. Distler [a], Eleanor D. Lederer [a,b,c], Barbara J. Clark [d], Nicholas A. Delamere [e], Syed J. Khundmiri [a,b,c,*]

[a] Department of Medicine/Kidney Disease Program, University of Louisville, Louisville, KY, USA
[b] Department of Physiology, University of Louisville, Louisville, KY, USA
[c] Robley Rex Veterans Affairs Medical Center, Louisville, KY, USA
[d] Department of Biochemistry and Molecular Biology, University of Louisville, Louisville, KY, USA
[e] Department of Physiology, University of Arizona, Tucson, AZ, USA

ARTICLE INFO

ABSTRACT

Breast cancer is the second leading cause of death in women and thus has received a great deal of attention by researchers. Recent studies suggested decreased occurrence of cancer in patients treated with cardiac glycosides (CGs) for heart conditions. Because CGs induce their cellular effects via the Na^+, K^+ ATPase (Na–K), we treated four breast cancer cell lines (MCF-7, T47D, MDA-MB453, and MDA-MB231) and a non-cancerous breast ductal epithelial cell line (MCF-10A) with ouabain, a well-characterized CG, and measured cell proliferation by measuring bromodeoxyuridine incorporation. Ouabain (1 μM) decreased cell proliferation in all cell lines studied except MDA-MB453 cells. Western blot of Na–K α and β subunits showed α1, α3, and β1 expression in all cell lines except MDA-MB453 cells where Na–K protein and mRNA were absent. Potassium uptake, measured as rubidium (^{86}Rb) flux, and intracellular potassium were both significantly higher in MDA-MB453 cells compared to MCF-10A cells. RT-qPCR suggested a 7 fold increase in voltage-gated potassium channel (KCNQ2) expression in MDA-MB453 cells compared to MCF-10A cells. Inhibition of KCNQ2 prevented cell growth and ^{86}Rb uptake in MDA-MB453 cells but not in MCF-10A cells. All cancer cells had significantly higher vacuolar H-ATPase (V-ATPase) activity than MCF-10A cells. Inhibition of V-ATPase decreased ^{86}Rb uptake and intracellular potassium in MDA-MB453 cells but not in MCF-10A cells. The findings point to the absence of Na–K, high hERG and KCNQ2 expression, elevated V-ATPase activity and sensitivity to V-ATPase inhibitors in MDA-MB453. We conclude that cancer cells exhibit fundamentally different metabolic pathways for maintenance of intracellular ion homeostasis.

© 2013 Elsevier B.V. All rights reserved.

1. Introduction

As drug-resistant cancer has become more prevalent, so has the push to develop novel chemotherapeutics. Cardiac glycosides (CGs) have been used to treat malignancies dating back to the 8th century [1]. More recently, Stenkvist et al. [2,3] followed 175 patients in a 22.3 year case study with a breast carcinoma, where 32 were being treated with digitalis at the time of diagnosis. In the patients that were undergoing digitalis treatment, there was a significantly lower death rate compared to patients not treated with digitalis (6% vs. 34%). Additionally, digitalis patients exhibited a recurrence rate 9.6 times lower than non-digitalis patients [4]. Chen et al. [5] using an internal dose response analysis of data from 9271 patients with cardiac disease sex matched with controls from the Norwegian Cancer Registry demonstrated significant relationship between high plasma levels of digitoxin and a decreased risk for leukemia/lymphoma and kidney/urinary tract cancers.

CGs bind to and inhibit the Na^+, K^+ ATPase (Na–K), a heterotrimeric P-type ATPase consisting of α, β and γ-subunits. Na–K transports Na^+ and K^+ against their concentration gradients in a 3:2 stoichiometry. The gradients maintained by Na–K allow for the secondary transport of many organic and inorganic substances, osmotic regulation and ion homeostasis. Approximately 30% of the cell's resting energy consumption is due to the action of Na–K [4]. To date four isoforms of the α-subunit, three isoforms of the β-subunit and seven isoforms of the γ or FXYD subunit have been described [6]. Expression of the subunits is tissue specific, except for α1 and β1 which are ubiquitously expressed [7,8]. In addition to its pump functions, Na–K is now recognized as a scaffold to form a complex "signalosome" that activates several different signaling pathways such as the MAP kinase and PI3 kinase pathways. CGs elicit activation of signaling cascades in the cell that activates both pro-survival and pro-apoptotic pathways depending upon

* Corresponding author at: 570 S. Preston St., Donald Baxter Bldg. Room 102, University of Louisville, Louisville, KY 40202, USA. Tel.: +1 502 852 1160; fax: +1 502 852 4384.
E-mail address: syed.khundmiri@louisville.edu (S.J. Khundmiri).

the concentration and cell types. For example at low doses they activate pro-survival pathways in kidney cells [9] and at high doses activate caspases in cancer cells [10–13]. In rodent models CGs had no effect on cell proliferation while in monkey and human cancer cells they activate pro-apoptotic pathways [14].

Studies have found altered expression and activity of Na–K subunits in various cancers; e.g., colon, lung, and hepatocellular carcinoma. Sakai et al. demonstrated that an increased $\alpha3:\alpha1$ ratio occurs in colon tissue during normal to malignant transition [14,15]. Shibuya et al. suggest the upregulation of $\alpha3$ as the cause for increased pump activity and CG sensitivity in hepatocellular carcinoma [16]. In contrast, Mijatovic et al. [17] found that lung carcinomas overexpressing $\alpha1$ were more sensitive to certain CGs. Decreased β subunit expression has been observed in a number of cancers [18–20]. Na–K β subunits are involved in cell to cell interactions, and decreased expression has been reported for a number of cancers implicating a possible role in epithelial to mesenchymal transformation that is seen in malignancies [5,18–20]. These differential alterations in Na–K expression in cancer cells may account for the differential sensitivity reported for CGs, possibly through disruption of the Na–K "signalosome" [14,17].

The present study examines the effect of CGs on proliferation of breast cancer cells. Our data suggest that ouabain does not exert a preferential effect on cancer cell growth as it decreased cell proliferation in both cancerous and non-cancerous cells. In fact, we showed an increase in activity of vacuolar H^+-ATPase in cancer cells suggesting that this transport protein may be a more directed target for anticancer therapy than Na–K. Interestingly, we also demonstrated that the highly metastatic breast cancer line, MDA-MB453, did not express Na–K, relying instead on V-ATPase to maintain intracellular ion homeostasis.

2. Methods

2.1. Materials

All cell culture media and bovine serum were purchased from Invitrogen. PP2, LY290859, dofetilide, insulin, hydrocortisone, epidermal growth factor, and phosphatase and protease inhibitor cocktails were purchased from Sigma (St. Louis, MO). Ouabain, SCH28080, and 10, 10-bis (4-pyridinylmethyl)-9(10H)-anthracenone dihydrochloride (XE-991) were purchased from Tocris Bioscience (Ellisville, MO). BrdU cell proliferation kit was purchased from Abnova. mRNA isolation kit and mRNA to cDNA kit were purchased from Applied Biosystems. Taq DNA polymerase was purchased from BioRad. Quantitative PCR array kit, RT-profiler array for human neuroscience ion channels and transporters (catalog no. PAHS 036A) were purchased from SA Biosciences. Monoclonal antibodies against Na–K $\alpha1$ and $\beta1$ subunits were purchased from RBI-Sigma. Antibodies against Na–K $\alpha2$, $\alpha3$, and $\beta2$ were purchased from Upstate (Lake Placid, NY).

2.2. Cell culture

Experimental procedures were performed using MCF-10A, MCF-7 and MDA-MB453 (gifts from Dr. Roland Valdes, University of Louisville), T47D (a gift from Dr. Carolyn Klinge, University of Louisville) and MDA-MB231 cells (ATCC). The opossum kidney (OK) cells, a continuous cell line derived from Virginia opossum for mammalian renal proximal tubule [9] were a kind gift from Dr. Steven Scheinman (Health Sciences Center, Syracuse, NY). The estrogen receptor expression status and tumorigenic characteristics of the cells are shown in Table 1. The MCF-10A, MCF-7 and MDA-MB231 cells were grown in media containing DMEM-F12 (1:1) supplemented with 5% fetal bovine serum (Invitrogen), 1% penicillin/streptomycin (Invitrogen), 834 µg/L insulin (Sigma), 0.5 µM hydrocortisone (Sigma) and 220 ng/L human epidermal growth factor (Sigma). The T47D and MDA-MB453 cells were maintained in RPMI 1640, supplemented with 5% FBS and insulin. OK cells were grown in Minimum Essential Medium with Earle's salts supplemented with 10% FBS and 1% penicillin/streptomycin.

2.3. Ouabain treatment

Stock ouabain (10 mM) was dissolved in DMSO and diluted in serum-free medium to get the required concentration as shown in Results. The final DMSO concentration was less than 0.1%. Unless otherwise stated, cells were treated with ouabain for 24 h at 37 °C in a humidified incubator (95% air/5% CO_2). Control cells were treated with 0.1% DMSO.

2.4. Cell proliferation assay

The cell lines were subcultured in 96-well plates at a density of 10,000 cells/well. Once the cells reach approximately 20% confluence, they were serum deprived (respective media supplemented with 1% serum) for 24 h, then treated with various concentrations of ouabain for 48 h. In the last 15 h of treatment, bromodeoxyuridine (BrdU) was added to the wells for incorporation into the DNA following manufacturer's instructions (BrdU ELISA kit, Abnova). The cells were fixed, washed, incubated with the monoclonal anti-BrdU primary antibody for 1 h at room temperature. The cells were washed and incubated for 30 min with HRP-conjugated secondary antibody. The absorbance measured at 450/540 nm is proportional to BrdU incorporation. The data are expressed as absorbance at 450/540 nm and analyzed by ANOVA followed by Bonferroni analysis.

2.5. Rubidium uptake

To assess potassium transport, ^{86}Rb uptake was performed as described previously [9]. Confluent serum deprived monolayers of breast cancer or MCF-10A cell lines grown on 24 well plates were

Table 1
Cells.

Cell Type	Organ	Disease	Tumorigenic	Metastatic	ER[a] +/−
MCF-10A	Mammary gland, breast	Fibrocystic disease	No	No	− [44,45]
MCF-7	Mammary gland, breast	Adenocarcinoma	Yes (with estrogen supplement)	Yes (pleural effusion)	+ [44,45]
T47D	Mammary gland, ductal tissue	Ductal carcinoma	Yes (with estrogen supplement)	Yes (pleural effusion)	+ [44,45]
MDA-MB231	Mammary gland, breast	Adenocarcinoma	Yes	Yes (pleural effusion)	− [44,45]
MDA-MBMB453	Mammary gland, breast	Metastatic carcinoma	No	Yes (involving nodes, brain, pericardial, pleural cavities)	− [44,45]
OK	Opossum kidney	None	No	No	+ [46]

[a] ER — estrogen receptor expression.

treated for 24 h with vehicle or 100 nM or 1 μM ouabain. Cells were incubated for 10 min in 1 μCi of ^{86}Rb, washed four times with PBS, and lysed overnight at 37 °C in a PBS containing 0.5 N NaOH and 0.1% Triton-X100. An aliquot of 100 μL of sample was used to measure radioactivity with scintillation counter and 50 μL of the sample was used to measure protein. The radioactivity counts were normalized to protein concentration. Rb uptake is expressed as nmoles Rb/mg protein/10 min or as percent change from the vehicle treated cells.

2.6. Measurement of cell sodium and potassium

Cell sodium or potassium was measured as described previously following the method described by Hou and Delamere [9,21]. The cell monolayers were washed with ice-cold isotonic magnesium chloride solution (100 mM MgCl$_2$, adjusted to pH 7.4 with Tris base). The magnesium chloride solution was removed and 200 μL of 30% nitric acid was added to each well to digest the cells. After this, 1.8 mL deionized water was added to each well and the sodium and potassium content of the diluted cell lysates was measured using an atomic absorption spectrophotometer (Perkin-Elmer, Norwalk, CT) at a wavelength of 566.5 nm. Intracellular sodium and potassium content is expressed as 10^{-9} mol/μg protein.

2.7. Crude membrane isolation

Cells were lysed in homogenization buffer containing 300 mM mannitol, 5 mM Tris-HEPES, and a 1:500 dilution of phosphatase and protease inhibitor cocktails (Sigma). Cell lysates were centrifuged at 780 ×g for 5 min to remove nuclei and cell debris. The supernatant was collected and centrifuged at 30,000 ×g for 45 min and the crude membrane pellet was resuspended in homogenization buffer by passing ten times through a 26 1/2 gauge needle. In some experiments nuclear free cell lysate was used to determine total Na–K ATPase expression in the control and cancer cells.

2.8. Western blot analysis

Western blots were performed as described previously [9].

2.9. mRNA isolation and RT PCR

mRNA was isolated from MCF-10A and MDA-MB453 cells grown in 75 cm^3 flasks using Ambion's mirVana™ mRNA Isolation Kit (Ambion catalog # AM1561) according to the manufacturer's protocol. Eluted RNA was stored overnight at −80 °C. RNA concentrations were determined using the DU730 Life Sciences UV/Vis Spectrophotometer (Beckman Coulter) and cDNA was synthesized using mRNA to cDNA kit (Applied Biosystems). Briefly, 4 μL high capacity RNA-to-cDNA Master Mix and 10 ng RNA template were added to a fresh PCR tube along with enough nuclease-free water for 20 μL total volume. Reverse transcription was performed using oligodT primers in Biorad MyCycler™ thermal cycler programmed to the following conditions: 37 °C − 1 h, 95 °C − 10 min, and 4 °C − 30 min. The cDNA samples were stored at −80 °C. PCR was performed in 20 μL volume containing 1 unit Biorad iProof™ High-Fidelity DNA polymerase, 5 mM MgCl$_2$, 1 mM dNTPs, and 200 nM each of forward and reverse primers specific for Na–K α1, α2, or α3 and 4 μL cDNA or water (negative control) at the following conditions: 98 °C − 1 min, (94 °C − 1 min, 50 °C − 1 min, 72 °C − 1 min) 35×, 72 °C − 5 min. The primer sequences for human Na–K α1 were GAAAGAAGTTTCTATGGA TG (forward) and ATGATTACAACGGCTGATAG (reverse, 318 bp product); for α2 were AGAGAATGGGGGCGGCAAGAAG (forward) and TGGTTCATCCTCCATGGCAGCC (reverse, 322 bp product); and for α3 were CCTCACTCAGAACCGCATGAC (forward) and TTCATCA CCAGCAGGTATCGG (reverse, 384 bp product). The PCR products were separated by 1% agarose gel electrophoresis and visualized using ethidium bromide. Data were analyzed by ImageQuant using Typhoon.

2.10. Quantitative RT-PCR

Total RNA was isolated as described above. RNA was reverse transcribed using oligodT primers as described above. Quantitative PCR was performed using RT-profiler array for human neuroscience ion channels and transporters (catalog no. PAHS 036A) and RT-SYBR green/ROX PCR master mix (catalog no. 330520, SA Biosciences, Frederick, MD) in Applied Biosystems 7500 quantitative PCR thermocycler according to the manufacturer's protocol. The transporters/channels are listed in Supplementary Table 1. Expression was quantified by the manufacturer's protocol as fold change relative to 18s RNA expression. Data were analyzed using SA Biosciences online software.

2.11. Bafilomycin A1 sensitive ATPase activity

Bafilomycin A1-sensitive ATP hydrolysis was assayed by measuring the production of inorganic phosphate as described previously [22] following the method described by Lu et al. [23]. Cells were lysed, crude membranes were prepared and ATPase activity was measured in the presence or absence of 1 mM bafilomycin A1, a maximal V-ATPase inhibitory concentration. Briefly, crude membranes were incubated in ATPase buffer containing 150 mM NaCl, 2 mM MgCl$_2$, 1 mM sodium vanadate, and 1 mM sodium azide (pH 6.75) for 15 min at room temperature in the presence and absence of 1 mM bafilomycin A1. The reaction was initiated by addition of ATP at a final concentration of 3 mM and incubated for 30 min at 37 °C. The reaction was stopped by addition of trichloroacetic acid. The samples were extracted with equal amount of chloroform to remove lipid and detergent. The samples were centrifuged at 10,000 rpm for 20 min at room temperature. The upper aqueous phase was transferred to clean test tubes and inorganic phosphate released was measured as described previously [22]. The difference in the ATPase activity assayed in the absence and presence of 1 mM bafilomycin A1 is taken as a measure of vacuolar H$^+$-ATPase activity. Vacuolar H$^+$-ATPase activity is expressed as μmoles Pi released per milligram protein per hour.

2.12. Protein determination

Protein concentration of samples was determined using a bicinchoninic acid protocol (Sigma) using bovine serum albumin as a standard.

2.13. Statistics

The data are presented as either SD or SEM where the n value represents the number of replicates. p values were obtained using GraphPad Prism software employing a two-way ANOVA followed by Bonferroni's post hoc analysis. Significance was established by a p value < 0.05.

3. Results

3.1. Cell morphology

To determine if ouabain changes cell morphology, cells were plated on 8-well glass chambers and treated for 24 h with 100 nM or 1 μM ouabain. As shown in Fig. 1, treatment with ouabain had no consistent effect on gross morphology in any of the cancer cell lines studied. However, treatment with 1 μM ouabain caused the MCF-10A cells to shrink and become rounded.
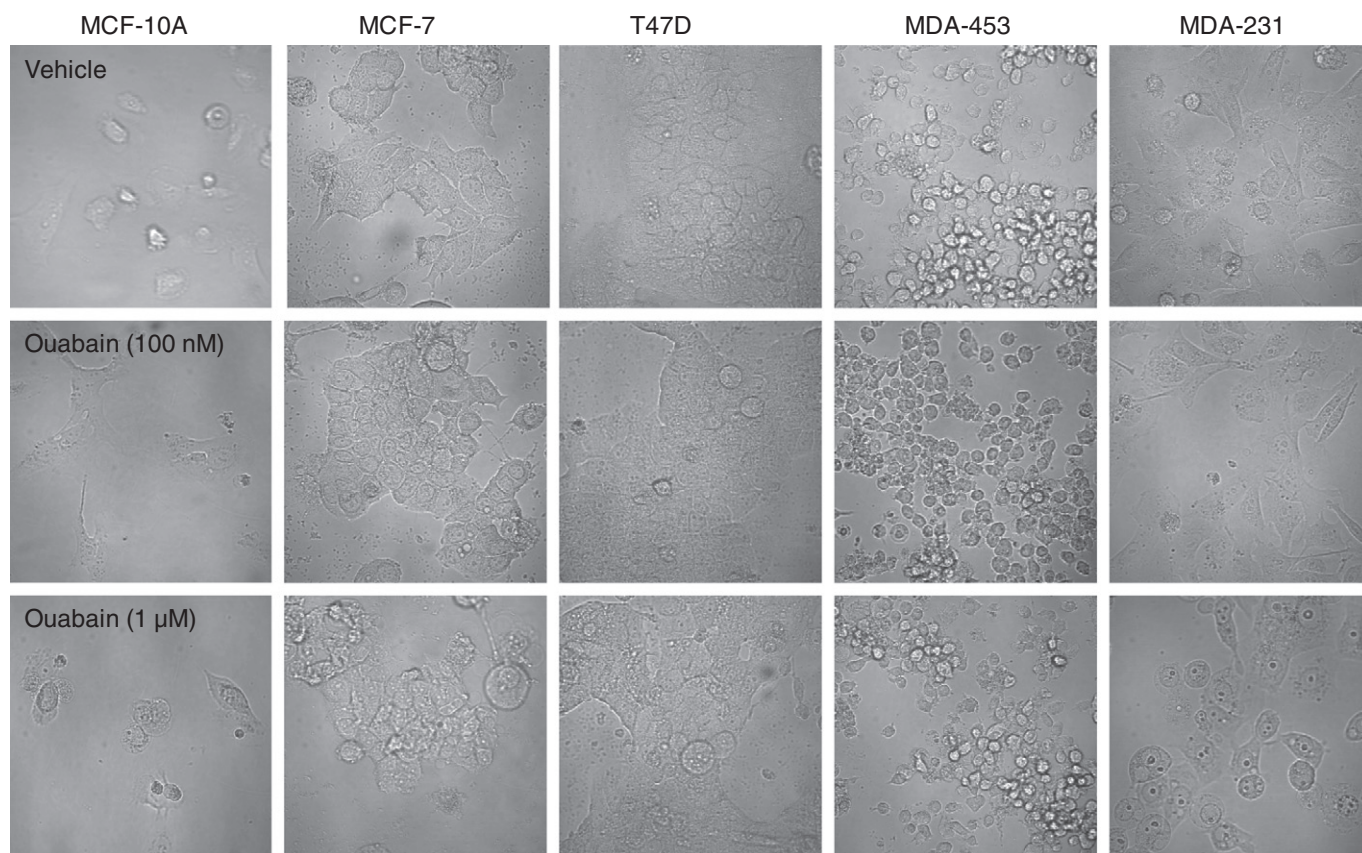
Fig. 1. Morphological features of breast cells. As described in Table 1, MCF-10A cells are non-cancerous from fibrocystic disease patient. MCF-7 and T47D cells are estrogen positive cells from breast carcinoma while MDA-MB231 and MDA-MB453 are estrogen negative cells from breast carcinoma. Cells were treated for 24 h with either 100 nM or 1 μM ouabain at 37 °C in a humidified 5% CO_2/95% air incubator. Transmission light microscopy was performed using Olympus FV1000 microscope using an oil immersion 60× objective lens.

3.2. Sensitivity of cancer cells to ouabain

To determine the effects of ouabain on cell proliferation, estrogen receptor positive (MCF-7 and T47D) and negative (MDA-MB453 and MDA-MB231) breast cancer cell lines and a non-cancerous, breast ductal epithelial cell line (MCF-10A) were treated for 0–4 days with 100 nM (a concentration close to IC50 for human Na–K α subunits) or 1 μM (an inhibitory concentration) ouabain. There was no significant inhibition of cell proliferation with 100 nM ouabain (Fig. 2A). Treatment with 1 μM ouabain decreased cell proliferation in all cell lines except MDA-MB453 cells by day 2 (Fig. 2B). Ouabain had no effect on cell proliferation in MDA-MB453 cells at either concentration.

3.3. Effect of ouabain on rubidium uptake

Because ouabain binds to and elicits its effects through Na–K [7], we tested the effects of 100 nM or 1 μM ouabain on total rubidium (^{86}Rb) uptake in MCF-10A and the four cancer cell lines. Treatment with 100 nM or 1 μM ouabain for 24 h significantly inhibited ^{86}Rb uptake in all cell lines except MDA-MB453 cells. Notably, ^{86}Rb uptake in the MDA-MB453 cancer cell line was two-fold greater than all the cells studied (Fig. 3A). MDA-MB453 cells had a significantly higher intracellular potassium concentration compared to MCF-10A cells (Fig. 3B). It is noteworthy that in both MCF-10A cells and MDA-MB453 cells sodium was roughly equivalent.

3.4. Na–K expression

The inability of ouabain at 1 μM concentration to inhibit proliferation of MDA-MB453 cells suggests that these cells might have an abnormal Na–K ATPase expression and function. Western blot analysis

of crude membrane preparations demonstrated an unexpected absence of all tested Na–K subunits in the MDA-MB453 cells (Fig. 4A–C). The MCF-10A, MCF-7, T47D and MDA-MB231 cell lines expressed the α1, α3 and β1 subunits of Na–K. The α2 and β2 subunits were not detectable in any of the cell lines (data not shown). The pattern of expression of NHE-1 was not unusual in any of the cells studied (Fig. 4D). To determine if the lack of Na–K expression in membrane was due to a trafficking defect, we performed Western blot on whole cell homogenates, and as shown in Fig. 4A–C (right panel) there was no detectable expression of any Na–K subunits in the MDA-MB453 cells. Additionally, there was a significant decrease in Na–K α1 expression in the T47D and MDA-MB231 cells, while the expression of Na–K α3 increased in the cancer lines relative to MCF-10A. The ratio of Na–K α3 to α1 was higher in MCF-7, T47D, and MDA-MB231 cells as compared to MCF-10A cells (Fig. 4E).

To further examine the apparent absence of Na–K protein expression, we isolated mRNA from MCF-10A and MDA-MB453 cells, and performed qualitative RT-PCR. As shown in Fig. 4F, MCF-10A cells expressed mRNA for Na–K α1 and α3 while there was no detectable Na–K α1 or α3 mRNA in MDA-MB453 cells.

Consistent with the lack of Na–K expression, evidence of Na–K dependent signaling cascade activation was absent in MDA-MB453 cells. As shown in Fig. 5, treatment for 15 min with 100 nM ouabain increased Src, ERK1/2, and Akt phosphorylation in MCF-10A cells but not in MDA-MB453 cells (Fig. 5). These data support the absence of a functional Na–K in MDA-453 cells.

3.5. SCH28080 sensitive ^{86}Rb uptake

The increased level of ^{86}Rb uptake in MDA-MB453 cells despite the absence of Na–K suggests that an alternative K$^+$ transport mechanism
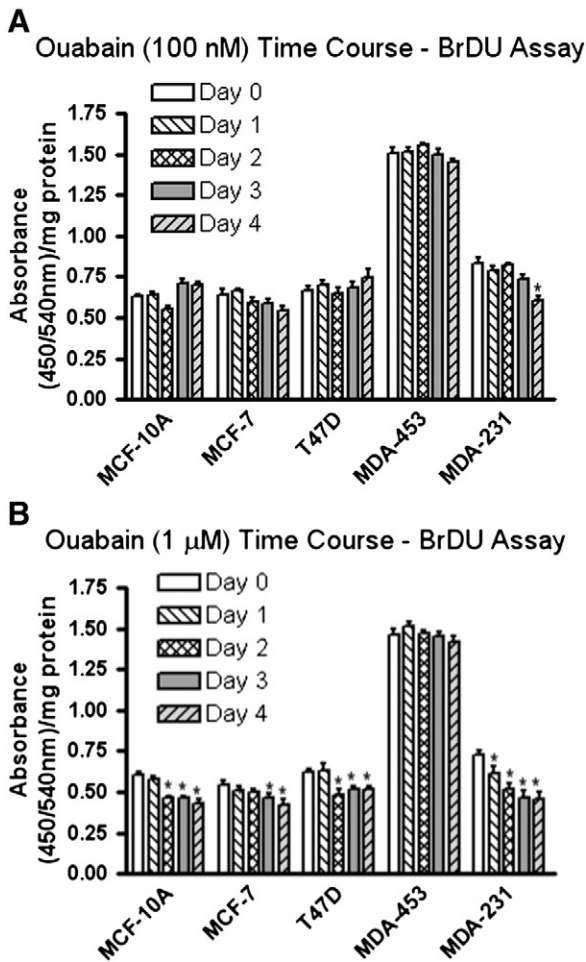
Fig. 2. Effect of ouabain on cell proliferation in breast cancer cells. Cells were treated with 100 nM (A) or 1 μM (B) ouabain for the indicated time. Cell proliferation was measured as BrdU incorporation in the DNA as described in Methods. Each bar represents data as mean ± se from 3 separate experiments (n = 3). In each experiment data was pooled from 12 repeats and the average was considered as one data point. * indicates significantly different (p < 0.05 by ANOVA) from the respective 0 day time point.

Fig. 3. Basal ^{86}Rb uptake and intracellular Na and K concentrations. A, cells were treated for 24 h with 100 nM or 1 μM ouabain and potassium uptake was measured as ^{86}Rb uptake in breast cancer cells. Each bar represents data as mean ± se from 4 separate experiments (n = 4). In each experiment data was pooled from 3 repeats and the average was considered as one data point. * indicates significantly different (p < 0.05 by ANOVA) from the respective vehicle (0) treated group. B, basal intracellular Na and K content was measured as described in Methods. The data are presented as 10^{-9} mol/μg protein. Each bar represents data as mean ± se from 3 separate experiments (n = 3). * indicates significantly different (p < 0.05 by ANOVA) from MCF-10A cells. Note logarithmic scale on y-axis in panel B.

is responsible for potassium (^{86}Rb) uptake. Because H$^+$–K$^+$ ATPase can bind ouabain and bears structural similarities to Na–K [24], we investigated the contribution of H$^+$–K$^+$ ATPase to K$^+$ transport in the breast cancer cells (Fig. 6A). By completely inhibiting Na–K using 10 μM ouabain, we determined that Na–K contributes approximately 50% of ^{86}Rb uptake in the MCF-10A, MCF-7 and MDA-MB231 cells; 75% in T47D cells; and 0% in MDA-MB453 cells. These findings are consistent with the total absence of Na–K protein and mRNA expression in MDA-MB453 cells. Inhibition of both gastric and non-gastric H$^+$–K$^+$ ATPase with 20 μM SCH28080 failed to inhibit ^{86}Rb uptake in any of the cell lines. Thus it is not likely that H$^+$–K$^+$ ATPase is a major contributor to K$^+$ transport in breast cancer cells. Similar results were obtained with omeprazole, a different inhibitor of H$^+$–K$^+$ ATPase (data not shown). Additionally, inhibition of NKCC with bumetanide had no effect on ^{86}Rb uptake (data not shown).

3.6. Ion channel/transporter qPCR array

To identify the potassium transporter/channel responsible for the increased ^{86}Rb uptake we performed ion channel/transporter qPCR array. Transporters increased in MDA-MB453 cells relative to MCF-10A are shown in Table 2. The expression of hERG (KCNH2, 14.78 fold), voltage-gated potassium channel of KQT subfamily member 2 (KCNQ2, 7.076 fold), inwardly-rectifying potassium channel (KCNJ4, 4.678 fold),
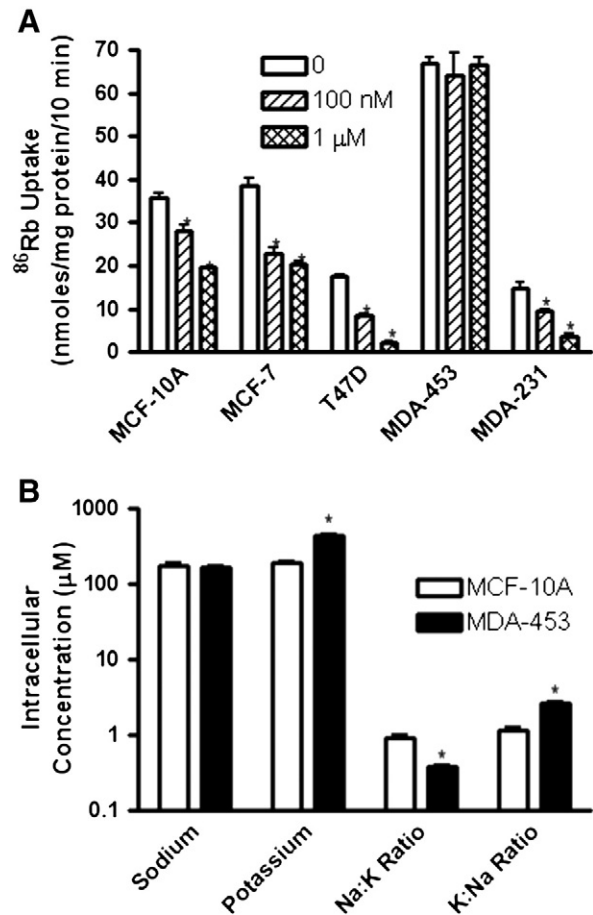
voltage-gated potassium channel of Shab-related family (KCNB1, 3.613 fold), and Shaw-related subfamily (KCNC4, 3.161 fold) increased compared to MCF-10A cells. There was no differential expression of Na–K ATPase β1 subunit (ATP1B1, 1.21 fold), voltage-gated calcium channel (CACNA1A, 0.652 fold) and SLC6A3 (0.591) in MDA-MB453 cells. The expression of voltage-gated potassium channels of shaker-related family 1 (KCNA1, 0.0431 fold) and 4 (KCNA4, 0.218 fold), voltage-gated potassium channel G subfamily 1 (KCNG1, 0.0986 fold), voltage-gated potassium channel KQT subfamily 4 (KCNQ4, 0.0004 fold), and voltage gated sodium channel type IX (SCN9A, 0.145 fold) decreased compared to MCF-10A cells. Consistent with our Western blot data, Na–K α1 (0.0002 fold) was not detected in MDA-MB453 cells. It is noteworthy that, H$^+$, K$^+$ ATPase (ATP4A, 0.0006 fold) was undetectable in MDA-MB453 cells, consistent with lack of effect of SCH28080.

3.7. Dofetilide-sensitive ^{86}Rb uptake

The hERG channel is a voltage-gated K$^+$ channel found to have 14 fold increased mRNA expression in MDA-MB453 cancer cell lines as compared to the MCF-10A cells (Table 2) [25]. Wang et al. [26] demonstrated that ouabain at nanomolar concentrations inhibits hERG channel. We therefore, investigated the role of hERG using the specific hERG inhibitor, dofetilide, in ^{86}Rb uptake studies. We found a
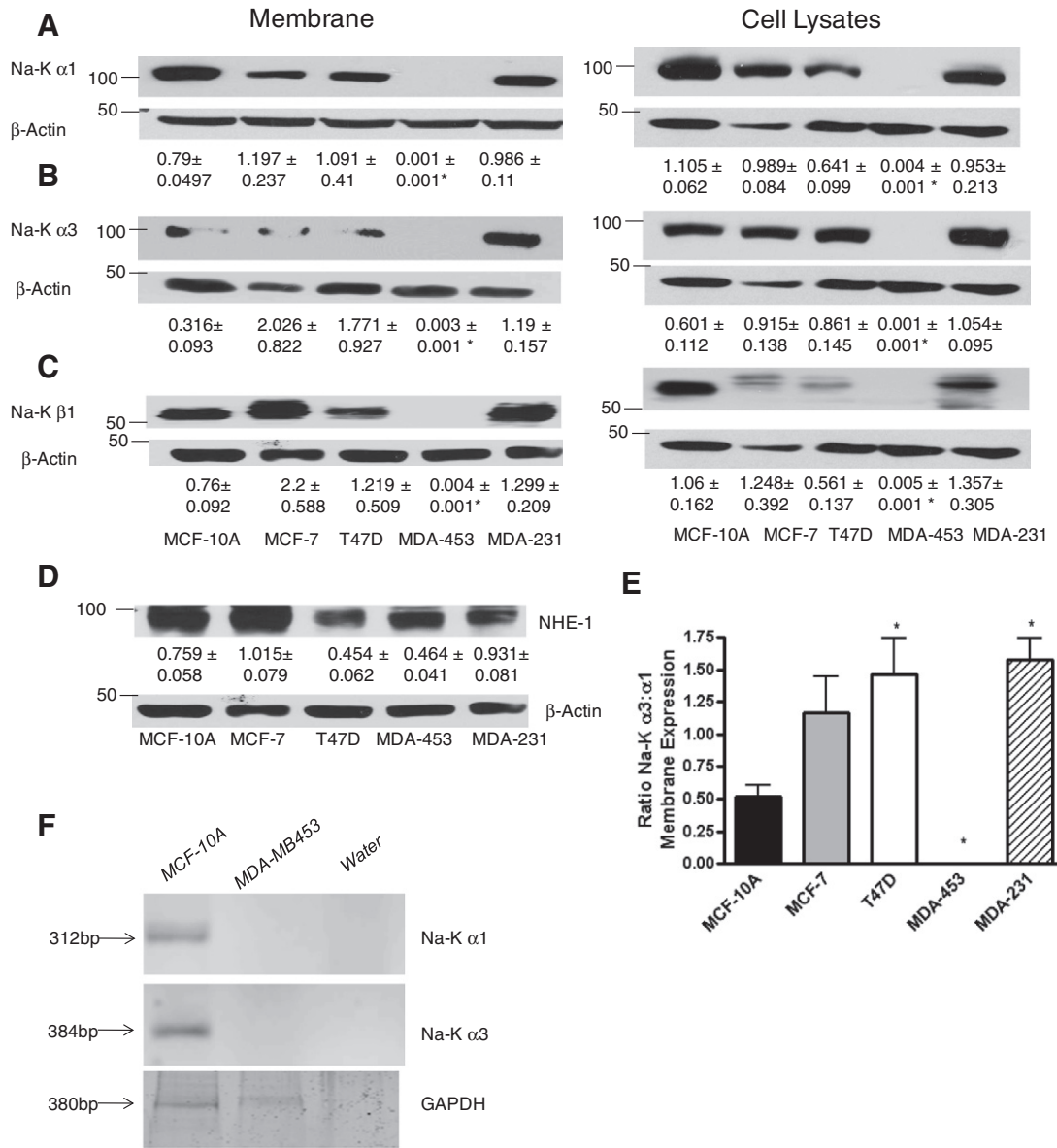
Fig. 4. Expression of Na–K ATPase in crude membranes and cell homogenates. Membrane expression of Na–K ATPase α1 subunit (A), α3 subunit (B), and β1 subunit (C) in crude membranes (left panel) or in homogenates (right panel). Expression of NHE-1 in crude membrane preparation (D). A representative Western blot is shown. Values mean ± se represent data as arbitrary units (ratio of protein expression to actin expression) from 4 separate experiments. * indicates significantly different (p < 0.05 by ANOVA) from the MCF-10A cells. E, ratio of Na–K α3:α1 membrane expression. Each bar represents mean ± se data as ratio of α3:α1 expression data from A and B. * indicates significantly different (p < 0.05 by ANOVA) from the MCF-10A cells. F, mRNA expression of Na–K α1 (upper panel) α3 (middle panel), and GAPDH (lower panel) was measured by RT-PCR as described in Methods. Representative gel from 4 different experiments is shown.

significant decrease in ^{86}Rb uptake upon dofetilide treatment in non-cancerous MCF-10A cells only (Fig. 6B). Dofetilide had no effect on ^{86}Rb uptake in any cancer line tested. This indicates that the hERG channel is not likely to contribute to potassium flux (^{86}Rb uptake) in MDA-MB453 cells.

3.8. Effect of KCNQ2 inhibition on cell proliferation

Because the increase in KCNQ2 expression was higher (7.3 fold) than the other potassium channels except hERG, we examined the role of KCNQ2 in cell proliferation and ^{86}Rb uptake in MCF-10A and MDA-MB453 cells. Cells were treated for 24 h or 48 h with a specific KCNQ2 inhibitor (8 μM XE-991, IC50 800 nM) and cell proliferation and ^{86}Rb uptake were measured. As shown in Fig. 7A, treatment with XE-991 had a small but significant effect on cell proliferation in MDA-MB453 cells but not in MCF-10A cells. ^{86}Rb uptake was also

partially inhibited by XE-991 in MDA-MB453 cells but not in MCF-10A cells (Fig. 7B).

3.9. Vacuolar ATPase (V-ATPase) activity

Because the V-ATPase proton pump is electrogenic it could feasibly establish electrical potential in cells that lack Na–K expression [27–29]. To examine V-ATPase activity we determined bafilomycin-sensitive ATP hydrolysis in crude membrane preparations of the breast cancer cells and compared the activity with renal proximal tubule (OK) cells from opossum kidney. As shown in Fig. 8, all breast cell lines had a significantly higher V-ATPase activity compared to kidney cells. Basal V-ATPase activity in crude membrane preparations was significantly higher in all cancer cell lines as compared to non-cancerous MCF-10A cells. To determine if V-ATPase provides sufficient electrical potential to drive potassium uptake in MDA-MB453 cells, ^{86}Rb uptake was
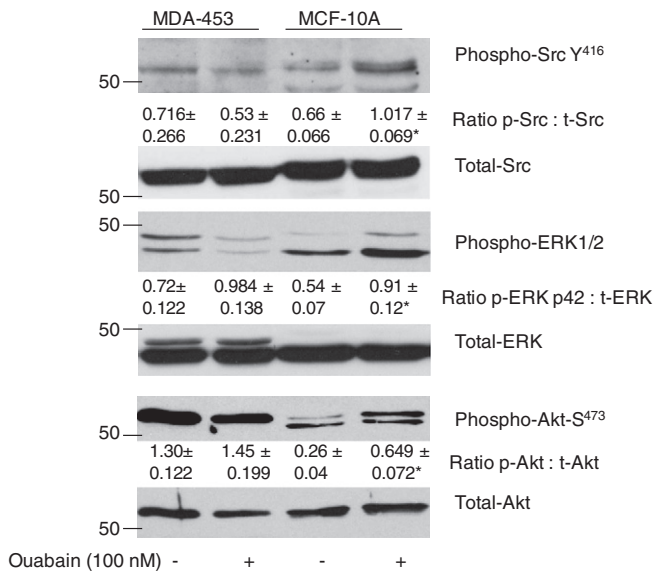
Fig. 5. Effect of ouabain on Src, ERK, and Akt phosphorylation. Cells were treated for 15 min with 100 nM ouabain, lysed in buffer containing 50 mM mannitol, 5 mM Tris-HEPES pH 7.4, 0.1% Triton X-100, 0.5% SDS, 0.5% NP40, and 10 μL/100 μL phosphatase and protease cocktails, and centrifuged at 14,000 ×g for 15 min. Supernatant proteins (50 μg/lane) were separated by 10% SDS-PAGE, transferred to nitrocellulose membranes. Proteins were detected using phospho-specific antibodies. Membranes were stripped and reprobed with antibodies to total proteins. A representative Western blot from 4 independent experiments is shown. Values mean ± se represent data as arbitrary units (ratio of phospho-protein expression to total protein expression) from 4 separate experiments. * indicates significantly different ($p < 0.05$ by ANOVA) from the vehicle treated cells.

measured in cells treated for 30 min or 24 h with 170 nM bafilomycin A1 or 50 nM concanamycin A. As shown in Fig. 9A, 24 h treatment with bafilomycin A1 or concanamycin A completely abolished ^{86}Rb uptake (Fig. 9A, upper panel). The same bafilomycin A1 and concanamycin A treatment caused a very large decrease in intracellular potassium content (Fig. 9B, upper panel). Interestingly, 30 min treatment with bafilomycin A1 or concanamycin A had no effect on ^{86}Rb uptake (Fig. 9A, lower panel).

4. Discussion

In the present study, we demonstrate a remarkable variability in the expression of transport proteins involved in the maintenance of intracellular ion homeostasis in a series of benign and malignant breast epithelial cells, with correlation to phenotypic features. We identified a two-fold greater potassium uptake and intracellular potassium content, a complete absence of Na–K expression both at the protein and mRNA level, and increased vacuolar H^+-ATPase activity in a highly metastatic cell line, MDA-MB453 cells, compared to a non-cancerous breast epithelial cell line, MCF-10A and three other breast cancer cell lines. Our data also demonstrate that the increased potassium uptake and intracellular potassium in MDA-MB453 cells is dependent upon the electrical potential driven by vacuolar H^+-ATPase. The other three breast cancer cells lines also exhibited variability in their expression of the Na–K subunits but all three showed an increase in vacuolar ATPase activity relative to the benign cell line.

As would be predicted from these findings, ouabain had no anti-proliferative activity against MDA-MB453 cells but showed variable antiproliferative effects on all of the other cells lines, both benign and cancerous. Moreover, we show that ouabain does not specifically decrease cell proliferation in cancer cells and its effect did not correlate with the ER status or tumorigenicity. The cell lines most susceptible to the anti-proliferative effects of ouabain were T47D, an ER positive, tumorigenic, and metastatic cell and MDA-MB231, an ER negative,
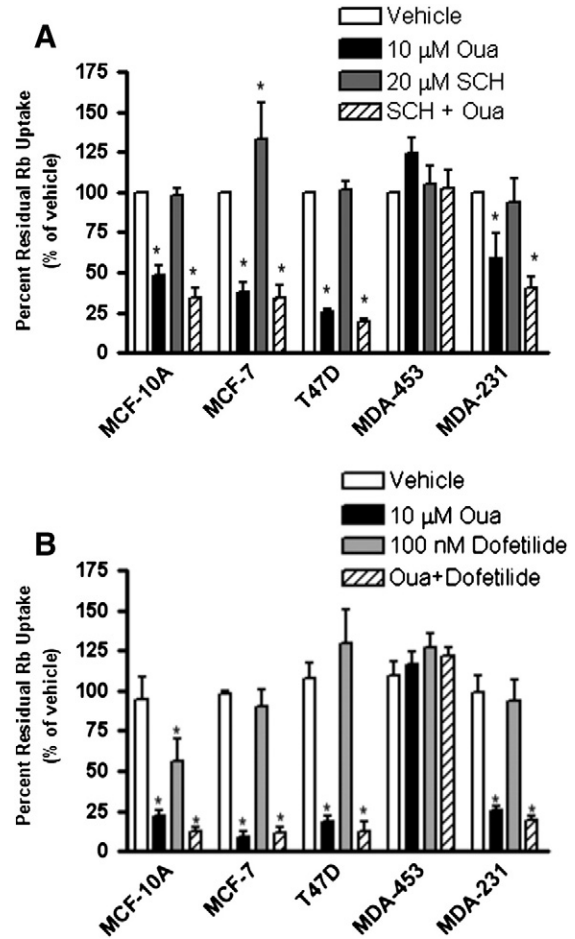

Fig. 6. Effect of H^+–K^+ ATPase and hERG on total ^{86}Rb uptake. Cells were treated for 24 h with 20 μM SCH28080, an H^+–K^+ ATPase inhibitor (A) or 100 nM dofetilide, an inhibitor of hERG (B). Total potassium uptake was measured as ^{86}Rb uptake as described in Methods. Each bar represents data as mean ± se percent residual uptake from vehicle treated group from 3 individual experiments (n = 3). In each experiment data from 4 repeats was averaged and considered as one data point. * indicates significantly different ($p < 0.05$ by ANOVA) from the respective vehicle treated group.

tumorigenic and metastatic cell. Our data demonstrate a differential effect of the cardioglycoside, ouabain, on multiple breast cancer cell lines relative to a non-cancerous cell line, MCF-10A. Ouabain at a lower concentration (100 nM) had no effect on cell proliferation in any of the cell lines studied. At higher concentrations (1 μM), inhibition of

Table 2

Expression of different ion channels in MDA-MB453 cells as compared to MCF10A cells.

Protein	Fold expression levels from MCF-10A
ATP1A1 (Na–K ATPase α1)	0.0002
ATP1B1 (Na–K ATPase β1)	1.2101
ATP4A (H–K ATPase)	0.0006
CACNB3	3.2009
CFTR	0.0004
CLCA1	0.0003
CLCNC3	0.3779
CLCNC6	7.1384
KCNA1	0.0431
KCNB1	3.16133
KCNC4	2.1807
KCNH4 (hERG)	14.7823
KCNJ4	4.67839
KCNQ2	7.0763
SLC2A1 (GLUT1)	11.9853
SLC18A2	3.8605

(A complete list of ion transporters is presented as Supplementary Table 2.)(A complete list of ion transporters is presented as Supplementary Table 2.)
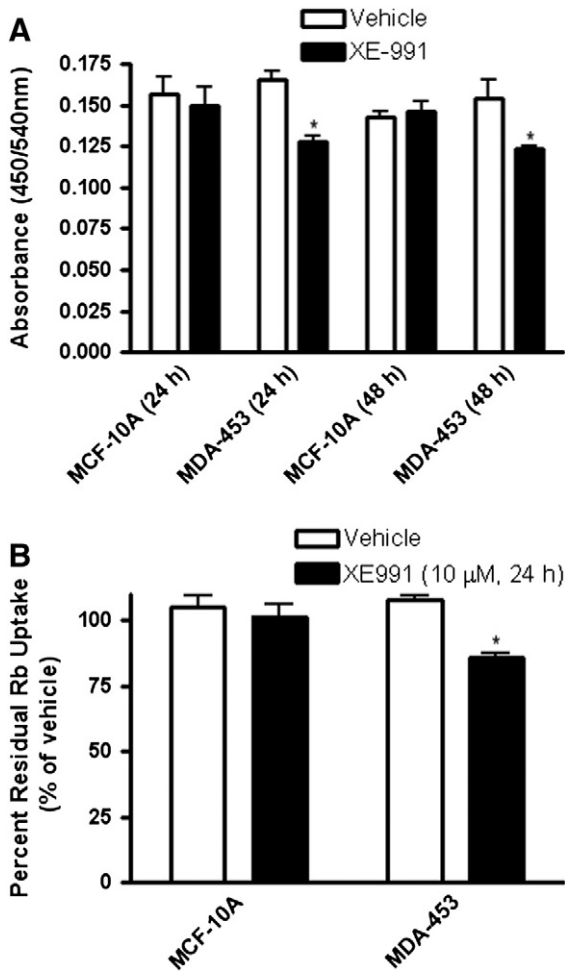
Fig. 7. Effect of KCNQ2 on cell proliferation and ^{86}Rb uptake. MCF-10A or MDA-MB453 cells were treated with XE991, an inhibitor of KCNQ2 for 24 or 48 h. Cell proliferation (A) or total potassium uptake as ^{86}Rb uptake (B) was measured as described in Methods. Each bar represents data as mean ± se from 3 individual experiments (n = 3). In each experiment data from 4 repeats was averaged and considered as one data point. * indicates significantly different (p < 0.05 by ANOVA) from the respective vehicle treated group.
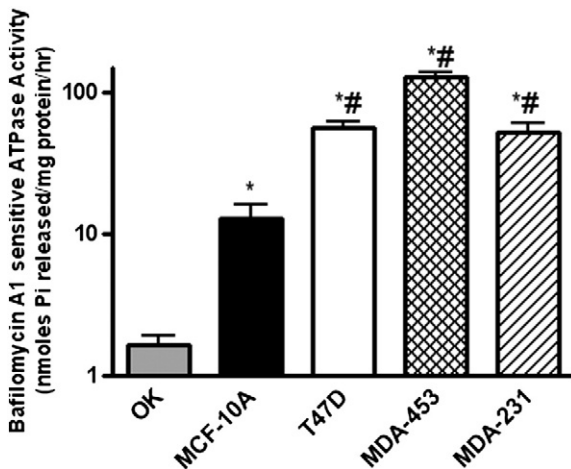

Fig. 8. Basal V-ATPase activity. V-ATPase activity was measured as bafilomycin A1 (1 mM)-sensitive ATP hydrolysis as described in Methods. Each bar represents data as mean ± se from 3 individual experiments (n = 3). Each experiment was performed in triplicate and the data were averaged and considered as one data point. * indicates significantly different (p < 0.05 by ANOVA) from activity in OK cells and # indicates significantly different (p < 0.05 by ANOVA) from activity in MCF-10A cells.

cell proliferation was similar in both cancer and non-cancerous cells with the exception of MDA-MB453 cells consistent with lack of Na–K expression.

The absence of Na–K expression in the MDA-MB453 cells raises the question of how these cells maintain normal intracellular homeostasis. Intracellular K content was higher in MDA-MB453 cells than in MCF-10A, but the content of Na was similar. The very high K flux as demonstrated by ^{86}Rb uptake studies suggested a unique mechanism for maintenance of intracellular ion balance. Because of the similarities between Na–K and H$^+$–K$^+$ ATPase [24], we initially hypothesized that this P type ATPase was responsible for the K uptake; however, inhibitor studies did not support this supposition. Quantitative RT-PCR analysis showed the lack of H$^+$, K$^+$ ATPase expression in these cells consistent with the lack of SCH28080 effect on ^{86}Rb uptake. In a recent study Wang et al. [26] demonstrated that hERG can bind to ouabain; however, inhibition of this inward rectifying potassium channel by dofetilide had no effect on ^{86}Rb uptake in any of the cancer cell lines studied. The lack of effect of dofetilide on ^{86}Rb uptake in all the cancer cells may be explained by the fact that hERG generally permits the passive movement of potassium ions out of the cell. Interestingly, however, inhibition of ^{86}Rb uptake in non-cancerous MCF-10A cells by dofetilide may suggest that inhibition of hERG reduces the rate of potassium exit causing the cell to suppress active potassium uptake in order to maintain steady state. Our study for the first time suggests overexpression of the potassium channel KCNQ2 in highly metastatic ER negative breast cancer cells (MDA-MB453). Inhibition of KCNQ2 partially suppressed cell proliferation and ^{86}Rb uptake in MDA-MB453 cells but not in MCF-10A cells suggesting that KCNQ2 is responsible for at least some of the enhanced Rb flux.

In eukaryotic cells V-ATPase energizes the transport of H$^+$ ions into the vacuoles and lysosomes for organelle acidification. Using pharmacological inhibitors and RNAi several studies demonstrated the importance of plasma membrane V-ATPase in metastasis, cell proliferation, pH homeostasis, and invasion in breast cancer cells [30–35]. Our data showed significantly higher V-ATPase activity in crude membrane preparations from cancer cells compared to non-cancerous cells. Interestingly, media from a day old culture of MDA-MB453 cells were very highly acidic (data not shown), suggesting preferential localization of V-ATPase to the plasma membrane. The decrease in ^{86}Rb uptake and intracellular potassium in cells treated with specific V-ATPase inhibitors, bafilomycin A1 and concanamycin A supports the notion that the V-ATPase may establish the electrical potential required for transport of potassium in the cancer cells. Providing the cells have a reasonably high input resistance, the electrogenic, outwardly directed, active proton transport by V-ATPase would give rise to a negative membrane potential that would favor K channel-mediated potassium accumulation. The absence of an immediate effect in 30 min, however, also raises the possibility that additional mechanisms for maintenance of the high Rb flux may exist.

The absence of all subunits of the Na–K in the MDA-MB453 cell line may be a critical observation in understanding metastasis in cancer cells. Our data supports the work from Rajasekaran's laboratory [18–20] that demonstrated the loss of Na–K in epithelial to mesenchymal transformation and metastasis. The absence of Na–K may explain the loss of cell–cell contact, morphology, and the highly metastatic nature of these cells and could be an adaptation of cells to escape the regulation by endogenous cardiac glycosides. Our findings are at odds with Einbond et al. [36] who reported that treatment with the cardiac glycoside-like compound actein inhibited cell proliferation by a mechanism that required activation of Src, Akt and Erk2 in MDA-MB453 cells. The authors suggested that actein acted through inhibition of Na–K. While they did indeed observe Na–K activity inhibition caused by actein, the ATPase assay was performed using a kit that contains kidney microsomes which would be expected to express Na–K in high abundance. Considering the absence of Na–K in MDA-MB453 cells and the high concentration of actein and digitoxin
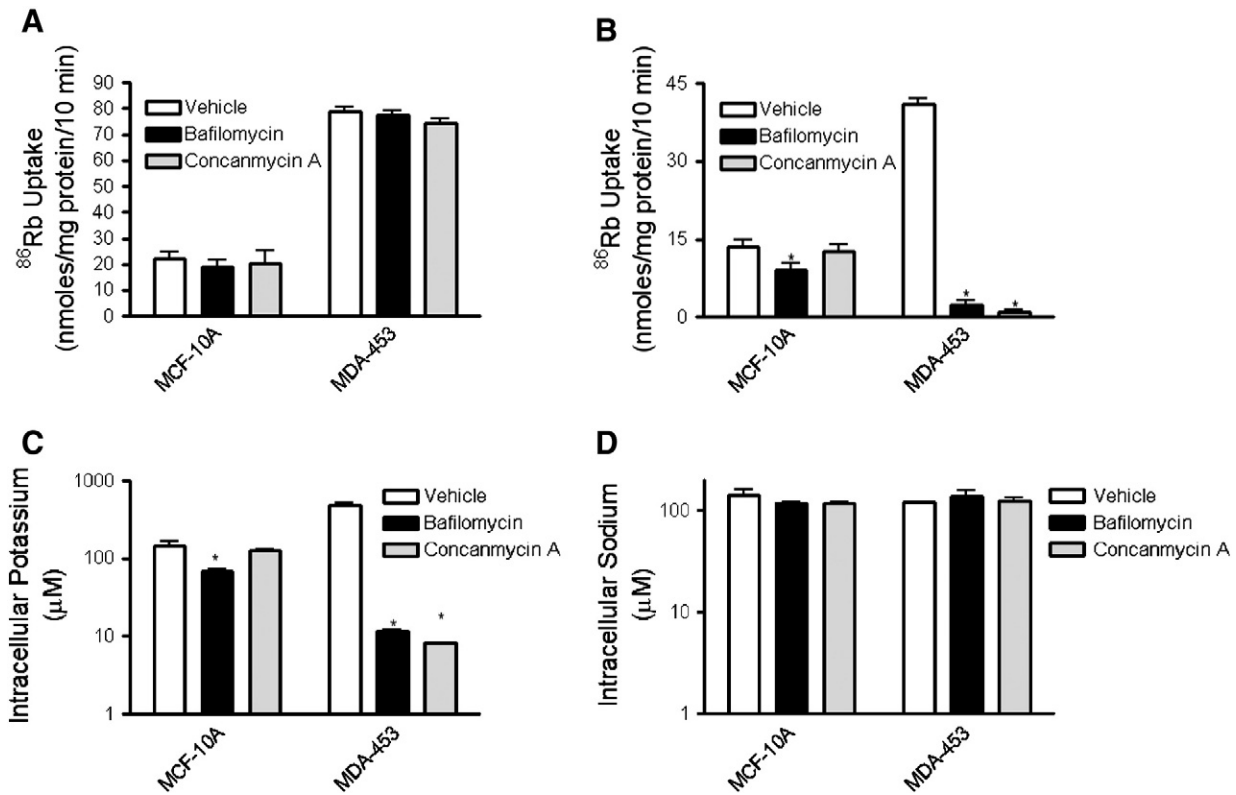
Fig. 9. Effect of V-ATPase inhibition on total ^{86}Rb uptake and intracellular Na and K concentrations. Cells were treated with 170 nM bafilomycin A1 or 50 nM concanamycin A for 30 min (A) or 24 h (B–D) and total ^{86}Rb uptake (A and B) or intracellular K (C) or Na (D) were measured as described in Methods. Each bar represents data as mean $\pm$ se from 3 individual experiments (n = 3). Each experiment was performed in triplicate and the data was averaged and considered as one data point. * indicates significantly different (p < 0.05 by ANOVA) from respective vehicle treated cells. Note logarithmic scale on y-axis in panels C and D.

($>$100 μM) required to elicit a response, it seems plausible that the effects of actein may not be linked to Na–K.

Several studies have demonstrated an inhibitory effect of cardiac glycosides on a variety of cancers, including breast cancer, but have not included comparison to non-cancerous cell lines [14,37–43]. We were able to reproduce this inhibitory effect on the MCF-7, T47D, and MDA-MB231 breast cancer cell lines, as well as the non-cancerous MCF-10A cell line at 1 μM ouabain. Notably, lower concentration of ouabain (100 nM) had no effect on cell proliferation in any of the cell lines studied. However, we also observed a widely variable sensitivity of the various cancer cell lines to the anti-proliferative effect of high doses of ouabain. The basis for this variable response is not apparent but our data would suggest that the presence or absence of the ER is not a discriminating factor in determining ouabain sensitivity. The differences in sensitivity to ouabain may lie in the observation that the cell lines most sensitive to ouabain, T47D and MDA-MB231 cells, had higher Na–K α3 to α1 subunit ratio.

In summary, our data demonstrates for the first time the absence of Na–K in ER negative highly metastatic cancer cells, MDA-MB453, which occurs in parallel with high V-ATPase activity and high hERG and KCNQ2 potassium channel expression. The findings suggest that for certain tumors V-ATPase and other potassium channels like KCNQ2 may be a target for cancer therapy. In the other breast cancer cells, which do express Na–K, the antiproliferative effect of ouabain was significant but not more pronounced than in non-cancer cells. It is noteworthy that breast cancer cells exhibit significant heterogeneity in the expression of transport proteins responsible for maintenance of intracellular homeostasis. These differences suggest the presence of fundamental differences in cancer cell metabolism that could potentially be exploited for the development of new therapies for breast cancer. The differences in the Na–K subunits and the lack of cancer cell selectivity

for the antiproliferative effects of ouabain suggest that the application of ouabain-like cardioglycosides for breast cancer may be limited.

Supplementary data to this article can be found online at http://dx.doi.org/10.1016/j.bbadis.2013.04.023.

References

[1] H. Brewer, Historical perspectives on health. Early Arabic medicine, J. R. Soc. Health 124 (2004) 184–187.

[2] B. Stenkvist, E. Bengtsson, O. Eriksson, J. Holmquist, B. Nordin, S. Westman-Naeser, G. Eklund, Cardiac glycosides and breast cancer, Lancet 313 (1979) 563.

[3] B. Stenkvist, Is digitalis a therapy for breast carcinoma? Oncol. Rep. 6 (1999) 493–496.

[4] I. Prassas, E.P. Diamandis, Novel therapeutic applications of cardiac glycosides, Nat. Rev. Drug Discov. 7 (2008) 926–935.

[5] J.Q. Chen, R.G. Contreras, R. Wang, S.V. Fernandez, L. Shoshani, I.H. Russo, M. Cereijido, J. Russo, Sodium/potassium ATPase (Na$^+$, K$^+$-ATPase) and ouabain/related cardiac glycosides: a new paradigm for development of anti-breast cancer drugs? Breast Cancer Res. Treat. 96 (2006) 1–15.

[6] G. Blanco, Na, K-ATPase subunit heterogeneity as a mechanism for tissue specific ion regulation, Semin. Nephrol. 25 (2005) 292–303.

[7] J.B. Lingrel, The physiological significance of the cardiotonic steroid/ouabain-binding site of the Na, K-ATPase, Annu. Rev. Physiol. 72 (2010) 395–412.

[8] T. Mijatovic, E. Van Quaquebeke, B. Delest, O. Debeir, F. Darro, R. Kiss, Cardiotonic steroids on the road to anti-cancer therapy, Biochim. Biophys. Acta 1776 (2007) 32–57.

[9] S.J. Khundmiri, M.A. Metzler, M. Ameen, V. Amin, M.J. Rane, N.A. Delamere, Ouabain induces proliferation through calcium-dependent phosphorylation of Akt (protein kinase B) in opossum kidney proximal tubule cells, Am. J. Physiol. Cell Physiol. 291 (2006) C1247–C1257.

[10] Y. Sreenivasan, P.B. Raghavendra, S.K. Manna, Oleandrin mediated expression of Fas potentiates apoptosis in tumor cells, J. Clin. Immunol. 26 (2006) 308–322.

[11] F. Mollinedo, C. Gajate, Fas/CD95 death receptor and lipid rafts: new targets for apoptosis-directed cancer therapy, Drug Resist. Updat. 9 (2006) 51–73.

[12] D.J. McConkey, Y. Lin, L.K. Nutt, H.Z. Ozel, R.A. Newman, Cardiac glycosides stimulate Ca2$^+$ increases and apoptosis in androgen independent, metastatic human prostate adenocarcinoma cells, Cancer Res. 60 (2000) 3807–3812.

[13] R.A. Newman, Y. Kondo, T. Yokoyama, S. Dixon, C. Cartwright, D. Chan, M. Johansen, P. Yang, Autophagic cell death of human pancreatic tumor cells mediated by oleandrin, a lipid-soluble cardiac glycoside, Integr. Cancer Ther. 6 (2007) 354–364.

[14] R.A. Newman, P. Yang, A.D. Pawlus, K.I. Block, Cardiac glycosides as novel cancer therapeutic agents, Mol. Interv. 8 (2008) 36–49.

[15] H. Sakai, T. Suzuki, M. Maeda, Y. Takahashi, N. Horikawa, T. Minamimura, K. Tsukada, N. Takeguchi, Upregulation of NaK alpha3 and downregulation of alpha1 in human colorectal cancer, FEBS Lett. 563 (2004) 151–154.

[16] K. Shibuya, J. Fukuoka, T. Fujii, E. Shimoda, T. Shimizu, H. Sakai, K. Tsukada, Increase in ouabain-sensitive K$^+$-ATPase activity in hepatocellular carcinoma by overexpression of Na$^+$, K$^+$-ATPase alpha 3-isoform, Eur. J. Pharmacol. 638 (2010) 42–46.

[17] T. Mijatovic, U. Jungwirth, P. Heffeter, M.A. Hoda, R. Dornetshuber, R. Kiss, W. Berger, The Na$^+$/K$^+$-ATPase is the Achilles heel of multi-drug-resistant cancer cells, Cancer Lett. 282 (2009) 30–34.

[18] L.J. Inge, S.A. Rajasekaran, K. Yoshimoto, P.S. Mischel, W. McBride, E. Landaw, A.K. Rajasekaran, Evidence for a potential tumor suppressor role for the Na, K-ATPase beta1-subunit, Histol. Histopathol. 23 (2008) 459–467.

[19] S.A. Rajasekaran, T.P. Huynh, D.G. Wolle, C.E. Espineda, L.J. Inge, A. Skay, C. Lassman, S.B. Nicholas, J.F. Harper, A.E. Reeves, M.M. Ahmed, J.M. Leatherman, J.M. Mullin, A.K. Rajasekaran, Na, K-ATPase subunits as markers for epithelial–mesenchymal transition in cancer and fibrosis, Mol. Cancer Ther. 9 (2010) 1515–1524.

[20] S.A. Rajasekaran, A.K. Rajasekaran, Na, K-ATPase and epithelial tight junctions, Front. Biosci. 14 (2009) 2130–2148.

[21] Y. Hou, N.A. Delamere, Influence of ANGII on cytoplasmic sodium in cultured rabbit nonpigmented ciliary epithelium, Am. J. Physiol. Cell Physiol. 282 (2002) C552–C559.

[22] A. Ahmad, S.J. Khundmiri, F. Pribble, M.L. Merchant, M. Ameen, J.B. Klein, M. Levi, E.D. Lederer, Role of vacuolar ATPase in the trafficking of renal type IIa sodium-phosphate cotransporter, Cell. Physiol. Biochem. 27 (2011) 703–714.

[23] M. Lu, S. Vergara, L. Zhang, L.S. Holliday, J. Aris, S.L. Gluck, The amino-terminal domain of the E subunit of vacuolar H(+)-ATPase (V-ATPase) interacts with the H subunit and is required for V-ATPase function, J Biol Chem. 277 (2002) 38409–38415.

[24] K. Munson, R.J. Law, G. Sachs, Analysis of the gastric H,K ATPase for ion pathways and inhibitor binding sites, Biochemistry 46 (2007) 5398–5417.

[25] V. Asher, H. Sowter, R. Shaw, A. Bali, R. Khan, EAG and hERG potassium channels as novel therapeutic targets in cancer, World J. Surg. Oncol. 8 (2010) 113.

[26] L. Wang, B.A. Wible, X. Wan, E. Ficker, Cardiac glycosides as novel inhibitors of human ether-a-go-go-related gene channel trafficking, J. Pharmacol. Exp. Ther. 320 (2007) 525–534.

[27] G. Strompen, J. Dettmer, Y.-D. Stierhof, K. Schumacher, G. Jurgens, U. Maye, Arabidopsis vacuolar H$^+$-ATPase subunit E isoform 1 is required for Golgi organization and vacuole function in embryogenesis, Plant J. 41 (2005) 125–132.

[28] S. Padmanaban, X. Lin, I. Perera, Y. Kawamura, H. Sze, Differential expression of vacuolar H-ATPase subunit c genes in tissues active in membrane trafficking

[29] H. Wieczorek, G. Gruber, W.R. Harvey, M. Huss, H. Merzendorfer, The plasma membrane H$^+$-V-ATPase from tobacco hornworm midgut, J. Bioenerg. Biomembr. 31 (1999) 67–74.

[30] S.R. Sennoune, K. Bakunts, G.M. Martinez, J.L. Chua-Tuan, Y. Kebir, M.N. Attaya, R. Martinez-Zaguilan, Vacuolar H$^+$ ATPase in human breast cancer cells with distinct metastatic potential: distribution and functional activity, Am. J. Physiol. Cell Physiol. 286 (2004) C1443–C1452.

[31] P. McHenry, W.W. Wang, E. Devitt, N. Kluesner, V.J. Davisson, E. McKee, D. Schweitzer, P. Helquist, M. Tenniswood, Iejimalides A and B inhibit lysosomal vacuolar H$^+$-ATPase (V-ATPase) activity and induce S-phase arrest and apoptosis in MCF-7 cells, J. Cell. Biochem. 109 (2010) 634–642.

[32] H. You, H. Jin, H. Shu, B. Yu, A.D. Milito, F. Lozupone, Y. Deng, N. Tang, G. Yao, S. Fais, J. Gu, W. Qin, Small interfering RNA targeting the subunit ATP6L of proton pump V-ATPase overcomes chemoresistance of breast cancer cells, Cancer Lett. 280 (2009) 110–119.

[33] T. Morimura, K. Fujita, M. Akita, M. Nagashima, A. Satomi, The proton pump inhibitor inhibits cell growth and induces apoptosis in human hepatoblastoma, Pediatr. Surg. Int. 24 (2008) 1087–1094.

[34] A. Hinton, S.R. Sennoune, S. Bond, M. Fang, M. Reuveni, G.G. Sahagian, D. Jay, R. Martinez-Zaguilan, M. Forgac, Function of a subunit isoforms of the V-ATPase in pH homeostasis and in vitro invasion of MDA-MB231 human breast cancer cells, J. Biol. Chem. 284 (2009) 16400–16408.

[35] C. Daniel, C. Bell, C. Burton, S. Harguindey, S. Reshkin, C. Rauch, The role of proton dynamics in the development and maintenance of multidrug resistance in cancer, Biochim. Biophys. Acta 1832 (2013) 606–617.

[36] L.S. Einbond, M. Shimizu, H. Ma, H.A. Wu, S. Goldsberry, S. Sicular, M. Panjikaran, G. Genovese, E. Cruz, Actein inhibits the Na$^+$–K$^+$-ATPase and enhances the growth inhibitory effect of digitoxin on human breast cancer cells, Biochem. Biophys. Res. Commun. 375 (2008) 608–613.

[37] A. Svensson, F. Azarbayjani, U. Bäckman, T. Matsumoto, R. Christofferson, Digoxin inhibits neuroblastoma tumor growth in mice, Anticancer Res. 25 (2005) 207–212.

[38] K. Winnicka, K. Bielawski, A. Bielawska, A. Surazyński, Antiproliferative activity of derivatives of ouabain, digoxin and proscillaridin A in human MCF-7 and MDA-MB231 breast cancer cells, Biol. Pharm. Bull. 31 (2008) 1131–1140.

[39] P. Kometiani, L. Liu, A. Askari, Digitalis-induced signaling by Na$^+$/K$^+$-ATPase in human breast cancer cells, Mol. Pharmacol. 67 (2005) 929–936.

[40] E.B. LeWinn, Cardiac glycosides and breast cancer, Lancet 1 (1979) 1196–1197.

[41] Y. Lin, D.H. Ho, R.A. Newman, Human tumor cell sensitivity to oleandrin is dependent on relative expression of Na$^+$, K$^+$-ATPase subunits, J. Exp. Ther. Oncol. 8 (2010) 271–286.

[42] P. Yang, D.G. Menter, C. Cartwright, D. Chan, S. Dixon, M. Suraokar, G. Mendoza, N. Llansa, R.A. Newman, Oleandrin-mediated inhibition of human tumor cell proliferation: importance of Na,K-ATPase alpha subunits as drug targets, Mol. Cancer Ther. 8 (2009) 2319–2328.

[43] Z. Li, Z. Zhang, J.X. Xie, X. Li, J. Tian, T. Cai, H. Cui, H. Ding, J.I. Shapiro, Z. Xie, Na/K-ATPase mimetic pNaKtide peptide inhibits the growth of human cancer cells, J. Biol. Chem. 285 (2011) 32394–32403.

[44] R.M. Neve, K. Chin, J. Fridlyand, J. Yeh, F.L. Baehner, T. Fevr, L. Clark, N. Bayani, J.-P. Coppe, F. Tong, T. Speed, P.T. Spellman, S. DeVries, A. Lapuk, N.J. Wang, W.-L. Kuo, J.L. Stilwell, D. Pinkel, D.G. Albertson, F.M. Waldman, F. McCormick, R.B. Dickson, M.L. Johnson, S. Ethier, A. Gazdar, J.W. Gray, A collection of breast cancer cell lines for the study of functionally distinct cancer subtypes, Cancer Cell 10 (2006) 515–527.

[45] D.L. Holliday, V. Speirs, Choosing the right cell line for breast cancer research, Breast Cancer Res. 13 (2011) 215, (http://breast-cancer-research.com/content/13/4/215).

[46] J.L. Stock, J.A. Coderre, E.M. Burke, D.B. Danner, S.D. Chipman, J.R. Shapiro, Identification of estrogen receptor mRNA and the estrogen modulation of parathyroid hormone-stimulated cyclic AMP accumulation in opossum kidney cells, J. Cell. Physiol. 150 (1992) 517–525.